Workshop on Visualisation in Environmental Sciences (EnvirVis) (2018)
R. Bujack and K. Rink and D. Zeckzer and S. Jänicke (Editors)

Change Point Detection for Ocean Eddy Analysis

D. Banesh[†1,2] , J. Wendelberger[2] , M. Petersen[2] , J. Ahrens[2] and B. Hamann[1]

[1]University of California Davis, U.S.A.
[2]Los Alamos National Laboratory, U.S.A.

Abstract

The detection and analysis of mesoscale ocean eddies is a complex task, made more difficult when simulated or observational ocean data are massive. We present the statistical approach of change point detection as a means to help scientists efficiently extract relevant scientific information. We demonstrate the value of change point detection for the characterization of eddy behavior in simulated ocean data. Our results show that change point detection helps with the identification of significant parameter values used in an algorithm or determination of time points that correspond to eddy activity of interest.

CCS Concepts

•***Mathematics of computing*** → ***Time series analysis; Exploratory data analysis;*** *Regression analysis;* •***Computing methodologies*** → *Object detection; Image processing;*

1. Introduction

Mesoscale ocean eddies are widely studied in ocean science. They are large, rotating bodies of water, ranging from 10km to 150km in diameter and are a vital component of the ocean's ecosystem. They influence the ocean's biological network [CGS*11], can contribute to heat transport over several hundred miles [VLF08], affect weather conditions in the ocean, and impact various other aspects of ocean dynamics [McW08].

Eddy detection and tracking is a complex task and a major part of mesoscale ocean eddy studies. A wide range of detection and tracking techniques have been explored. Chelton et al. [CSSdS07], Williams et al. [WPB*11] and Petersen et al. [PWM*13] employed variations of the Okubo-Weiss criterion to identify closed regions of uniform vorticity. Chaigneau et al. [CGG08] and Chen et al. [CHC11] used versions of a parameter-based, geometric streamline clustering method, the winding-angle method, to find closed streamlines. Souza et al. [SDBMLT11] compared the Okubo-Weiss and winding-angle approaches to a wavelet packet decomposition method (first introduced by Doglioli et al. [DBSL07]) to identify where one method might perform better than another. Though these techniques have been successful in the detection and tracking of eddies, oftentimes, in-depth analysis must be limited to smaller regions of the ocean or performed at coarser resolutions of the data than desired. Ocean simulation models are complex and time-consuming to generate, and simulations produce large amounts of data when executed at high resolutions [WPS*16]. In-situ and high-performance computing approaches might help a scientist to focus on regions and parameters of interest [AJO*14, WPS*16], but in-situ reduced datasets can still range from megabytes to gigabytes in size [BTP*17]. Parsing and exploring this data to find regions of scientific interest remains a challenging task.

Current applications of statistical techniques to eddy analysis focus on examining anomalies in the data from established trends or deviations from a known standard. In [CGG08], Chaigneau et al. derived the mean of various eddy attributes in Peru over the seasons. They determined the months with the most significant deviations from the averages in order to identify anomalies that might correspond to other oceanic activity at those times. Liu et al. [LCS*16] verified the accuracy of their eddy detection method, which was applied to various regions in the ocean, by comparing anomalies in their eddy statistics to anomalies in recorded measurements of the same ocean regions. Chen et al. [CHC11] found that strong inter-seasonal sea level variability in parts of the South China Sea correspond to higher than normal eddy numbers in the area. However, the statistical extent of many eddy-science papers are limited to average, standard deviation, and variance, where final conclusions are primarily made through guided visual inspection. Data collected over decades is averaged and graphed, after which an ocean scientist must painstakingly consider each time step to determine whether there are significant deviations from a predetermined standard. Techniques to automate this process, which would reduce the data a scientist must interactively examine, are highly desirable as they would greatly reduce effort and cost.

† We would like to thank Terece Turton and David Rogers for their time and support with this work. This work was funded by the Department of Energy at Los Alamos National Laboratory.

Given the complexities of ocean data, a tool to aid a scientist in more efficient exploration by intelligently reducing the search space, would be of significant benefit. We present a unique statistical approach, *change point detection*, for parameter and data analysis of ocean data, to guide a scientist to regions of interest. Based on criteria specified by the user, our method searches in a scientific dataset to identify points of interest. The resulting information can then be used to narrow the set of data to analyze and further refine the parameter space of a simulation. The techniques presented are general and can be used for simulation data, data captured by a satellite, data resulting from an in-situ method, or data stemming from other eddy analyses. Ocean analysis is a complex task and helping scientists find events from their large simulations can save valuable time and resources. The application of change detection to ocean data is a novel approach with broad implications.

Change point detection, or simply change detection, is a widely used statistical approach for targeted data reduction; it includes regression-based methods, Bayesian methods, and multi-variate methods, among others [BN*93]. Change detection techniques are used in various scientific disciplines. For example, Verbesselt et al. [VHNC10] examined satellite images showing land cover of vegetation over time to identify three types of events that might determine change: seasonal effects, gradual climate variability and abrupt change from deforestation, fires or floods. Myers et al. [MLF*16] applied change detection in-situ to a simulation of NASA's LCROSS project to identify time steps of significance. Jeon et al. [JSC16] used change detection to find the magnitude and frequency of extreme rainfall in areas around the world.

2. Methodology

A change point, in statistical terms, refers to a place or time such that the observed data follows one distribution up to that point and another distribution after that point [CG11]. Change point detection refers to a broad category of algorithms where the goal is to find change points in the data. Change detection algorithms generally serve two main purposes: (1) to decide whether there is change in the data and (2) to determine the locations where this change is present. For eddy detection and analysis, our goal with change point detection is to extract time steps of scientific significance, or identify important parametric values in the detection algorithm.

The method described in this section and exemplified in the following section is applied to ocean data derived from a Model for Prediction Across Scales-Ocean (MPAS-Ocean) [MD] simulation. This multi-resolution ocean simulation dataset with identifiable eddies, currents and other turbulent features is commonly used in the ocean science community [RPH*13]. From this ocean data, we extract Cinema image databases [AJO*14] of surface kinetic energy. A Cinema database is a collection of images, each image a perspective projection of the simulation data to a 2D image plane. When generating the Cinema database, the scientist must ensure the resolution of the images is sufficient enough for their future analysis, similar to how they must ensure the proper resolution of their original simulation. With this MPAS-Ocean Cinema dataset, we oversampled the simulation to ensure that each component of the simulation is represented by several pixels, ensuring a high quality of input for image feature analysis. We then apply the contour detection method described by Banesh et al. [BSAH17] to identify features of interest (Figure 1) from the Cinema databases. The contour detection technique takes the gray-scale version of a Cinema image as input. It applies a user-defined threshold value to assign all pixels in the image above the threshold to a value of one, and all pixels below the threshold to a value of zero. Every connected set of pixels with a value of one is considered to be a derived contour. The technique described is robust enough to track slow moving features over small deformations such as the curvature of the Earth's surface. Change detection analysis is applied to a metric based on these contours.

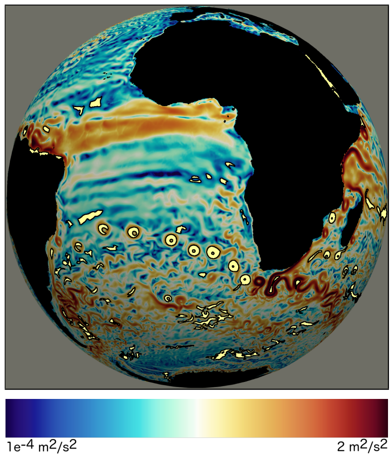

Figure 1: *MPAS-Ocean image from a Cinema database of surface kinetic energy, using a log-scale, hot-cold color-map (chosen for its perceptual advantages and minimal color vision issues [TWSR17]). Contour detection was applied with a threshold value of 77. Detected regions are highlighted in bright yellow.*

2.1. Change Detection

There are various categories of change detection algorithms based on various statistical concepts. We use a *piecewise linear regression model* based on the work presented by Myers et al. [MLF*16]. Although originally designed to analyze pixel values in an image, we have adapted this approach to detect changes in other types of data. There are a variety of change point methods based on piecewise representations, including the trend filtering approach proposed by Tibshirani [T*14] that uses the Lasso technique [HGT16].

A *linear regression model* estimates the least squares line fit to a set of data points. The goal is to estimate the best relationship between the dependent variable on the *x*-axis, and the independent variable on the *y*-axis. However, if the relationship between the two variables is non-linear, then the linear regression model will be a poor representation of the data. This can be addressed using a *piecewise* linear regression model, where line *segments* are fit to *subsets* of the data. A line segment is used to represent the data as long as the error between the data and the fitted line segment is acceptably small. When the addition of a new data point increases the error beyond the acceptable threshold, this point is set to be the "change point", where a new line segment begins (Figure 2).

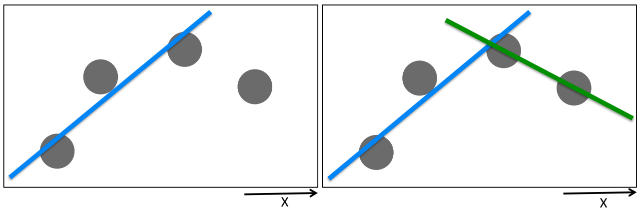

Figure 2: *Illustration of piecewise linear regression. The image on the left shows a blue line segment fit to the first three data points. The fourth point would introduce too much error to the linear regression model to be a good fit to the blue line. Therefore, a new line fit starts, as shown in green on the right, encompassing the third and fourth points. The fourth point is considered the change point.*

The piecewise linear regression model determines change points in the following way: The user first defines a buffer size, B, indicative of the number of data points the algorithm will consider to find a change point. For example, in a time-dependent data set, B would correspond to the number of time steps to examine. This approach ensures that even with very large data sets, calculations can still be performed efficiently by focusing on smaller regions when desired. Given a buffer size, B, the algorithm considers the first B time steps in the simulation, denoted as $curr$, and the subsequent B time steps, denoted as $buff$. It computes two residual sum-of-squares (RSS) terms for a piecewise linear fit; they are:

$$RSS_1 = RSS_{curr \cup buff}$$

$$RSS_2 = RSS_{curr} + RSS_{buff}$$

RSS_1 determines the RSS for the combined set of $curr$ and $buff$ (a single line was fit to the combination of both sets), while RSS_2 determines the sum of RSS for each set $curr$ and $buff$ (there were separate lines fit to $curr$ and to $buff$). These values are used to calculate the *F-statistic* associated with the two fits.

$$F = \frac{\left(\frac{RSS_1 - RSS_2}{p_2 - p_1}\right)}{\left(\frac{RSS_2}{T_{curr \cup buff} - p_2}\right)},$$

where $p_1 = 2$ and $p_2 = 4$, with p_1 and p_2 denoting the number of parameters in each fit; $T_{curr \cup buff}$ is the total number of time steps being considered. The F-statistic is used to determine whether one line or two lines would be a better representation for the selected region of data.

The user also provides a second input value, α. For any data point in $curr$ and $buff$, when the data point maps to a value of the F-distribution that is larger than the given α value, this point is considered to be a change point. For certain data sets, the α criterion for change point detection can still identify a larger number of change points than desired. Therefore, a third user-defined parameter is considered, δ^2. The F-distribution is closely related to the variance of the two sets of data, and because in most cases, closely located data are correlated with each other, the δ^2 parameter takes this correlation into account when detecting change points. This parameter directs the algorithm to make it more difficult to select change points in the presence of auto-correlation of nearby points. For more details on this piecewise linear regression model, see Section 3 of [MLF*16].

When applying this technique to eddy analysis data derived from our Cinema image databases of MPAS-Ocean, we found that these "more discrete" datasets resulted in more abrupt changes than the examples used in [MLF*16]. To address this issue, we added a wrapper function to the algorithm that first searches for regions in the data where two or more consecutive points have the same y-value; that is, flat regions of no change. The first data point of a flat region is automatically marked as a change point and the region of no change is marked as having no additional change points. The piecewise linear regression algorithm is applied to every set of remaining data points between these regions of no change to determine any additional change points in the data. We introduce an additional optional parameter, n_{flat}, ranging from two to $n+1$, where n is the size of the entire data set. Only flat regions above that number of points are considered and marked as having change points detected, with a value of $n+1$ indicating that a flat region, regardless of size, should not be considered. When searching large data sets, flat regions of two or three points might not necessarily indicate significant change, so this parameter allows a user to have control over the change points detected. Additionally, the first and last data points of a data set are always marked as change points.

As with most parameter-based eddy detection algorithms, including the Okubo-Weiss method, the winding-angle method and the 2D wavelet method [LCS*16], the image-based contour detection method presented in [BSAH17] requires a user to select a threshold parameter to identify features of interest. This can be a time-consuming process because a scientist must examine many parameter threshold values in order to identify those of significance. Using change point detection, a scientist can minimize this search space according to a scientifically relevant degree of change.

Figure 3 shows the results of the change detection algorithm applied to the contour threshold parameter of the contour detection algorithm presented in [BSAH17]. By holding the B and δ^2 values constant, we can vary the α value to identify various degrees of change. Figure 3(a) detects only the highest levels of change, from zero to the maximum number of features detected. Figures 3(b)-(d) gradually detect smaller levels of change until users can determine a level that fits their needs.

3. Results and Discussion

The data we examine in the previous section is a sample data set, included to illustrate the advantages of change detection for analysis techniques applied to ocean data. However, as seen in Figure 1, since the feature detection technique is applied to a color-mapped image, other turbulent structures in the ocean have also been detected as potential features of interest. For an eddy detection and tracking application, this leads to inaccurate results. To compute more precise results, in the case studies explored here, we apply our change detection algorithm to the "raw data" in a Cinema image database. In a raw data image, each pixel value is set to the value of the underlying MPAS-Ocean simulation it represents. It is not altered by a color-map or shading/lighting effects. Therefore, a

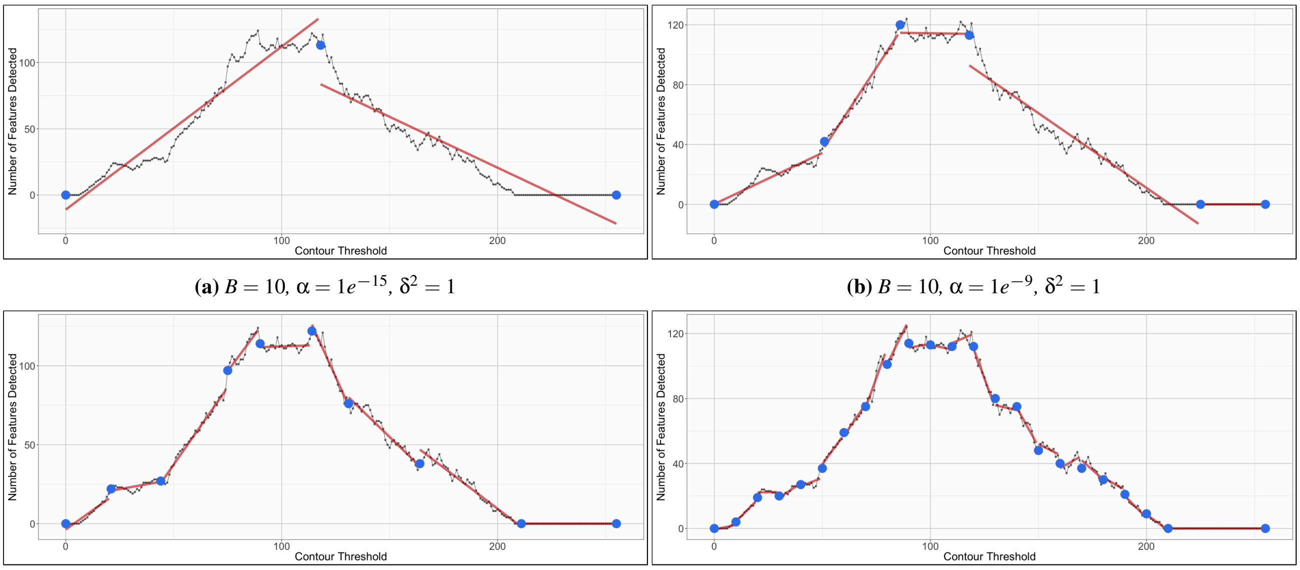

(a) $B = 10$, $\alpha = 1e^{-15}$, $\delta^2 = 1$ **(b)** $B = 10$, $\alpha = 1e^{-9}$, $\delta^2 = 1$

(c) $B = 10$, $\alpha = 1e^{-5}$, $\delta^2 = 1$ **(d)** $B = 10$, $\alpha = 1$, $\delta^2 = 1$

Figure 3: *Contour detection [BSAH17] applied to the MPAS-Ocean Cinema image shown in Figure 1. We vary the contour threshold value from 0 to 255 on the x-axis and plot the number of features detected on the y-axis. We apply change detection to this graph, holding B constant at 10 and δ^2 constant at 1, while varying α. The blue dots are the change points detected, and the red lines show the piecewise linear regression fits to the data. As α decreases, the number of change points decreases and only corresponds to the higher degrees of change in the data. As α increases, change points corresponding to smaller degrees of change are included.*

contour detection algorithm that is applied to this image provides a more accurate representation of the features present in the simulation. In the following case studies, we focus our attention on the eddies formed by the Agulhas Retroflection in the South Atlantic, also known as the Agulhas Rings, shown as the highlighted region in Figure 4).

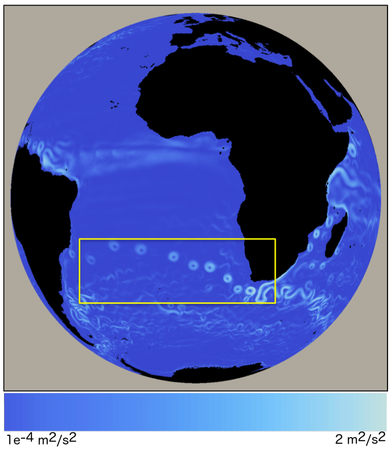

Figure 4: *MPAS-Ocean Cinema "raw data" image of kinetic surface energy. A log-scale, blue color-map is used for visualization purposes; actual analysis is conducted on the underlying data. The boxed region in yellow is the region of interest for our case studies.*

3.1. Case Study: Change Detection to Find Contour Threshold Parameter Values of Interest

To identify contour threshold parameter values of significance for eddies in the Agulhas Retroflection region, we apply change detection to the region selected in Figure 4. We vary the contour threshold parameter value from 0 to 255 on the x-axis and count the number of eddies detected on the y-axis. To analyze this data, we use the following change detection parameter values: $B = 4$, $\alpha = 5$, $\delta^2 = 1$, $n_{flat} = 2$.

The results are shown in Figure 5(a), with selected images corresponding to the 12 detected change points shown in Figure 5(b)-(g). When analyzing these results, we can make certain assessments of the data. The change point at contour threshold $(ct) = 4$ corresponds to the value where the major eddies of the Agulhas Rings are selected, including a few of the smaller meandering eddies and the eddies at the far right that are just about to be separated. Thresholds of $ct = 3$ and $ct = 5$ fail to find several eddies in this region. Starting from the change point at $ct = 8$ and moving up to $ct = 255$, every change point we detect corresponds to the start of a region of no change. In each of these regions, the eddies detected at the beginning of the flat regions remain the same until the end of the region. From these assessments, we can determine that the variation of the eddy detection algorithm over the 256 values of the contour threshold parameter range can be summarized by these 12 change points. We have effectively minimized the range of values a scientist needs to consider. Specifically, in the flat regions, as there is no

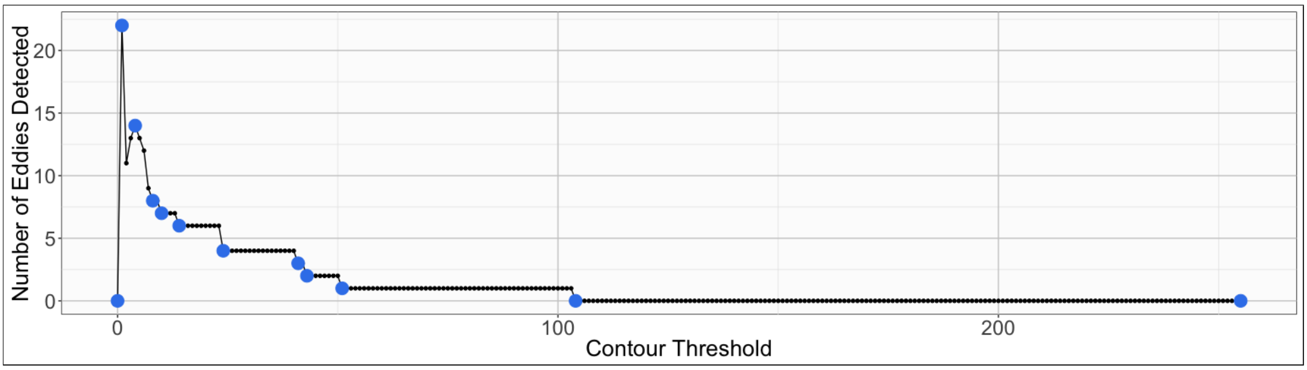

(a) $B = 4$, $\alpha = 5$, $\delta^2 = 1$, $n_{flat} = 2$

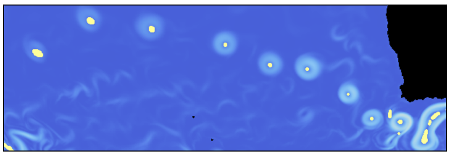

(b) *Contour Threshold = 4, Eddies Detected = 14*

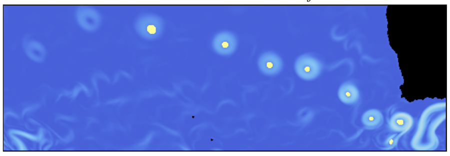

(c) *Contour Threshold = 8, Eddies Detected = 8*

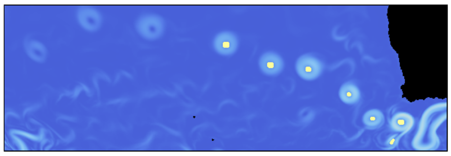

(d) *Contour Threshold = 10, Eddies Detected = 7*

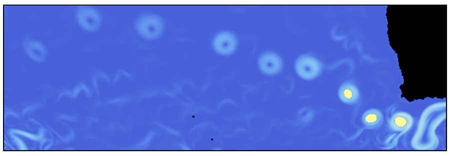

(e) *Contour Threshold = 41, Eddies Detected = 3*

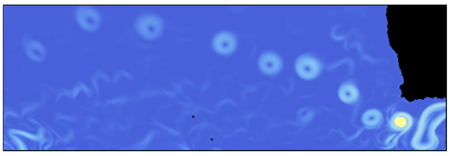

(f) *Contour Threshold = 51, Eddies Detected = 1*

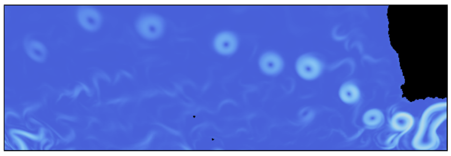

(g) *Contour Threshold = 104, Eddies Detected = 0*

Figure 5: *Eddy detection method applied to the selected region in Figure 4. In (a), change points are shown in blue. We vary the contour threshold parameter (x-axis) to identify eddies in the Agulhas Rings region (y-axis). The change point in (b) corresponds to the major eddies of the Agulhas Rings detected. In (c)-(g), in every flat region the eddies detected are the same; we simply lose a few eddies from one change point to the next.*

change in the eddies detected from start to end, an ocean scientist can save significant time.

3.2. Case Study: Change Detection to Find Time Steps of Interest

Finding change points in a time-dependent data set is one of the most common applications of statistical change detection. In this case study, we apply change detection to a time series of MPAS-Ocean Cinema "raw data" images for 60 time steps; each time step is five days apart. We remain focused on the region highlighted in Figure 4 and select a constant contour threshold value of 13. We iterate through time on the x-axis and count the number of eddies detected on the y-axis. We use the following change detection parameter values: $B = 3$, $\alpha = 1$, $\delta^2 = 1$, $n_{flat} = 2$.

The results of change detection applied to this data are shown in Figure 6. Here, we categorize our change points according to slope. When the slope from $timeStep(changepoint - 1)$ to $timeStep(changepoint)$ is positive, we mark the change point as green. When the slope is negative, we mark it as orange. All other change points are marked as blue. Of the 60 time steps analyzed, 10 are marked as change points with a positive slope. Change points with positive slope generally indicate the start of increased activity in this region. The two main types of increased activity occur when a new eddy separates from the Agulhas Retroflection or when one eddy splits into multiple eddies during its trek across the South Atlantic. Of these 10 positive-slope change points, we determined that six are time steps when a new eddy is separating from the Agulhas Retroflection, see Figure 6(b),(d). Visually, we determined that no false negatives are detected; we have not missed any time steps when a new eddy separates. Effectively, we have reduced the search space for a scientist from 60 time steps to 10.

3.3. Discussion

One of the most significant outcomes of this work was the realization of how novel it was to apply change detection to ocean science. Our ocean science collaborators were not familiar with the concept nor can it be found in oceanography literature. Since large time-dependent datasets are commonly found in both observational data and ocean simulation, applying statistical techniques such as change detection might lead to faster analysis or new insights. Our ocean science collaborators were excited to see the results presented here, and motivated to explore other areas of ocean science where change detection and other similar statistical approaches might impact their analysis.

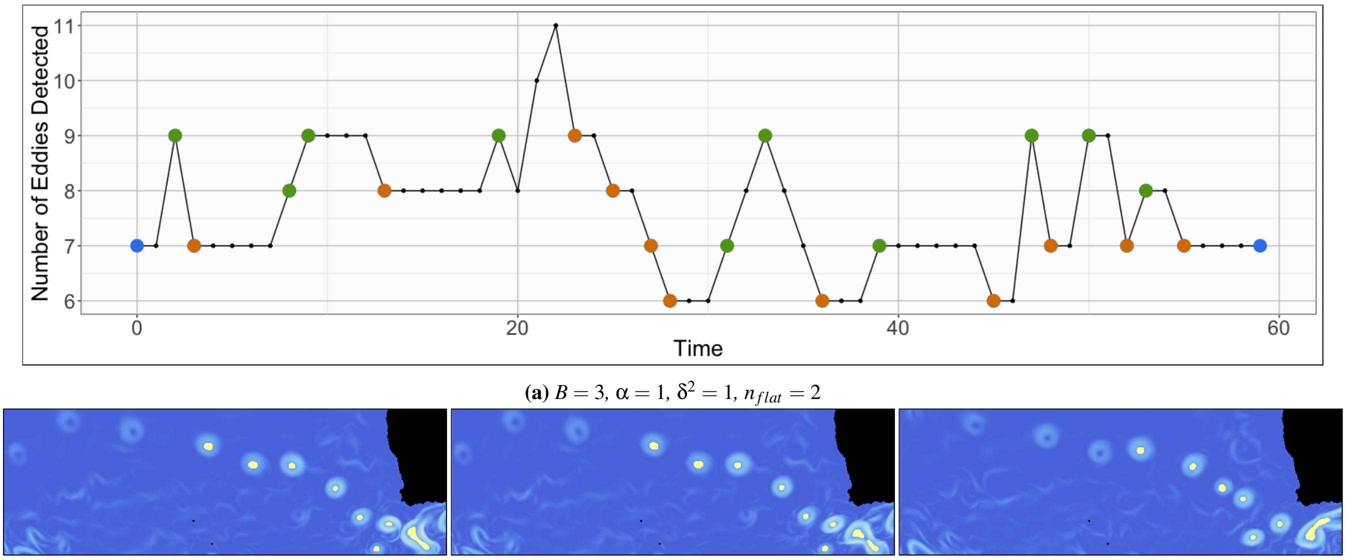

(a) $B = 3$, $\alpha = 1$, $\delta^2 = 1$, $n_{flat} = 2$

(b) *Time = 8, Eddies Detected = 8* **(c)** *Time = 9, Eddies Detected = 9* **(d)** *Time = 31, Eddies Detected = 7*

Figure 6: *Eddies are tracked in the Agulhas Retroflection region over 60 time steps. Change points are shown as a combination of blue, green and orange, where green change points indicate a positive slope from the previous step to the change point, orange indicates a negative slope, and blue indicates a zero slope. Green change points indicate the start of increased activity in the region: either a new eddy separates from the Agulhas Retroflection, as in (b) and (d), or one eddy splits into multiple eddies, as in (c).*

4. Conclusions

Eddy detection and tracking analysis is generally conducted using parametric methods, optimally over long periods of time. Tools that allow a scientist to process and analyze large amounts of data more efficiently must automate parameter space search and provide guidance on areas of scientific interest. We have presented a method that supports a scientist in this way, leading to a significant reduction in human effort. Our approach uses change detection as a valuable tool to help with the reduction of parameter search space, identifying just a subset(s) of the data to explore. We have provided two examples, one parameter-based and one time-based, supporting the advantages of our approach for scientific investigation of ocean data.

We are interested is testing this algorithm on other regions with high numbers of mesoscale eddies, such as the Kuroshio and Gulf Stream, as it might identify other scientifically meaningful eddy behavior. It would also be insightful to apply this technique to eddies at various ocean depths, and compare to the sea surface, as ocean behavior alters with depth. We also plan to extend this research to explore measurements captured from satellites and weather bouys in the ocean. A comparison to eddy census data, when available, would be useful to test the accuracy of our results. We also want to generalize this work by considering other metrics beyond the number of eddies. For example, we can consider birth, death, splitting and merging events of eddies. This would support scientific analysis of more specific activity within a region. Finally, we would like to devise and explore the use of multi-variate change point detection techniques, as they are likely to help with the identification of points of interest in multi-variate ocean data.

References

[AJO*14] AHRENS J., JOURDAIN S., O'LEARY P., PATCHETT J., ROGERS D. H., PETERSEN M.: An image-based approach to extreme scale in situ visualization and analysis. In *Proceedings of the International Conference for High Performance Computing, Networking, Storage and Analysis* (2014), IEEE Press, pp. 424–434. 1, 2

[BN*93] BASSEVILLE M., NIKIFOROV I. V., ET AL.: *Detection of abrupt changes: theory and application*, vol. 104. Prentice Hall Englewood Cliffs, 1993. 2

[BSAH17] BANESH D., SCHOONOVER J. A., AHRENS J. P., HAMANN B.: Extracting, Visualizing and Tracking Mesoscale Ocean Eddies in Two-dimensional Image Sequences Using Contours and Moments. In *Workshop on Visualisation in Environmental Sciences (EnvirVis)* (2017), Rink K., Middel A., Zeckzer D., Bujack R., (Eds.), The Eurographics Association. doi:10.2312/envirvis.20171103. 2, 3, 4

[BTP*17] BERRES A. S., TURTON T. L., PETERSEN M., ROGERS D. H., AHRENS J. P.: Video Compression for Ocean Simulation Image Databases. In *Workshop on Visualisation in Environmental Sciences (EnvirVis)* (2017), Rink K., Middel A., Zeckzer D., Bujack R., (Eds.), The Eurographics Association. doi:10.2312/envirvis.20171104. 1

[CG11] CHEN J., GUPTA A. K.: *Parametric statistical change point analysis: with applications to genetics, medicine, and finance*. Springer Science & Business Media, 2011. 2

[CGG08] CHAIGNEAU A., GIZOLME A., GRADOS C.: Mesoscale eddies off peru in altimeter records: Identification algorithms and eddy spatio-temporal patterns. *Progress in Oceanography 79*, 2-4 (2008), 106–119. 1

[CGS*11] CHELTON D. B., GAUBE P., SCHLAX M. G., EARLY J. J., SAMELSON R. M.: The influence of nonlinear mesoscale eddies on near-surface oceanic chlorophyll. *Science 334*, 6054 (2011), 328–332. 1

[CHC11] CHEN G., HOU Y., CHU X.: Mesoscale eddies in the south china sea: Mean properties, spatiotemporal variability, and impact on thermohaline structure. *Journal of Geophysical Research: Oceans 116*, C6 (2011). 1

[CSSdS07] CHELTON D. B., SCHLAX M. G., SAMELSON R. M., DE SZOEKE R. A.: Global observations of large oceanic eddies. *Geophysical Research Letters 34*, 15 (2007). 1

[DBSL07] DOGLIOLI A., BLANKE B., SPEICH S., LAPEYRE G.: Tracking coherent structures in a regional ocean model with wavelet analysis: Application to cape basin eddies. *Journal of Geophysical Research: Oceans 112*, C5 (2007). 1

[HGT16] HYUN S., G'SELL M., TIBSHIRANI R. J.: Exact post-selection inference for changepoint detection and other generalized lasso problems. *arXiv preprint arXiv:1606.03552* (2016). 2

[JSC16] JEON J.-J., SUNG J. H., CHUNG E.-S.: Abrupt change point detection of annual maximum precipitation using fused lasso. *Journal of Hydrology 538* (2016), 831–841. 2

[LCS*16] LIU Y., CHEN G., SUN M., LIU S., TIAN F.: A parallel sla-based algorithm for global mesoscale eddy identification. *Journal of Atmospheric and Oceanic Technology 33*, 12 (2016), 2743–2754. 1, 3

[McW08] MCWILLIAMS J. C.: The nature and consequences of oceanic eddies. *Ocean Modeling in an Eddying Regime* (2008), 5–15. 1

[MD] MPAS-DEVELOPERS: MPAS. http://mpas-dev.github.io/. (Accessed on 06/20/2016). 2

[MLF*16] MYERS K., LAWRENCE E., FUGATE M., BOWEN C. M., TICKNOR L., WOODRING J., WENDELBERGER J., AHRENS J.: Partitioning a large simulation as it runs. *Technometrics 58*, 3 (2016), 329–340. 2, 3

[PWM*13] PETERSEN M. R., WILLIAMS S. J., MALTRUD M. E., HECHT M. W., HAMANN B.: A three-dimensional eddy census of a high-resolution global ocean simulation. *Journal of Geophysical Research: Oceans 118*, 4 (2013), 1759–1774. 1

[RPH*13] RINGLER T., PETERSEN M., HIGDON R. L., JACOBSEN D., JONES P. W., MALTRUD M.: A multi-resolution approach to global ocean modeling. *Ocean Modelling 69*, Supplement C (2013), 211 – 232. URL: http://www.sciencedirect.com/science/article/pii/S1463500313000760, doi:https://doi.org/10.1016/j.ocemod.2013.04.010. 2

[SDBMLT11] SOUZA J. M. A. C. D., DE BOYER MONTEGUT C., LE TRAON P.-Y.: Comparison between three implementations of automatic identification algorithms for the quantification and characterization of mesoscale eddies in the south atlantic ocean. *Ocean Science 7*, 3 (2011), 317–334. 1

[T*14] TIBSHIRANI R. J., ET AL.: Adaptive piecewise polynomial estimation via trend filtering. *The Annals of Statistics 42*, 1 (2014), 285–323. 2

[TWSR17] TURTON T. L., WARE C., SAMSEL F., ROGERS D. H.: A crowdsourced approach to colormap assessment. In *EuroVis Workshop on Reproducibility, Verification, and Validation in Visualization (EuroRV3)* (2017), Lawonn K., Smit N., Cunningham D., (Eds.), The Eurographics Association. doi:10.2312/eurorv3.20171106. 2

[VHNC10] VERBESSELT J., HYNDMAN R., NEWNHAM G., CULVENOR D.: Detecting trend and seasonal changes in satellite image time series. *Remote sensing of Environment 114*, 1 (2010), 106–115. 2

[VLF08] VOLKOV D. L., LEE T., FU L.-L.: Eddy-induced meridional heat transport in the ocean. *Geophysical Research Letters 35*, 20 (2008). 1

[WPB*11] WILLIAMS S., PETERSEN M., BREMER P.-T., HECHT M., PASCUCCI V., AHRENS J., HLAWITSCHKA M., HAMANN B.: Adaptive extraction and quantification of geophysical vortices. *IEEE transactions on visualization and computer graphics 17*, 12 (2011), 2088–2095. 1

[WPS*16] WOODRING J., PETERSEN M., SCHMEIβER A., PATCHETT J., AHRENS J., HAGEN H.: In situ eddy analysis in a high-resolution ocean climate model. *IEEE transactions on visualization and computer graphics 22*, 1 (2016), 857–866. 1